Journal of Thermal Analysis and Calorimetry, Vol. 86 (2006) 3, 715–719

THE ROLE OF ALKALI CONTENT IN THE DEVITRIFICATION MECHANISMS OF SiO_2–Fe_2O_3–Na_2O–PbO SYSTEM*

*P. Kavouras, Th. Kehagias**, K. Chrissafis, Ph. Komninou and Th. Karakostas*

Physics Department, Aristotle University of Thessaloniki, 541 24 Thessaloniki, Greece

Three batch compositions of pure oxides (SiO_2, Fe_2O_3, PbO, Na_2O) with equivalent SiO_2, Fe_2O_3 and PbO contents and a gradually increased Na_2O content were vitrified through heating in a high temperature electric furnace and subsequent quenching. The resulting vitreous products were thermally treated in order to study the devitrification behaviour, under conditions designated from differential thermal analysis experiments. Depending on the Na_2O content, crystal phase separation gave rise to the growth of acmite and hematite or maghemite. A uniformly phase separated glass-ceramic material, with crystallites of similar size and population density, was produced from devitrification of the vitreous product with the higher Na_2O content.

Keywords: *electron microscopy, glass-ceramics, microhardness, microstructure, vitrification*

Introduction

We have used the vitrification method to stabilize hazardous solid residues, which originated from petrochemical distillery facilities [1] and mainly contained PbO and Fe_2O_3. The SiO_2–Fe_2O_3–Na_2O–PbO oxide system is a potential model system for the simulation of these vitrified solid wastes [2]. Hence, proper manipulation of the model system could result in finding the appropriate batch compositions that can be used for the fabrication of specific vitreous and glass-ceramic materials from the original solid waste.

A crucial aspect for the fabrication of glass-ceramics, generated by devitrification of the initial glasses, is the ability to control their final microstructure. In most cases, surface crystallisation should be avoided or depressed in favour of bulk crystallization [3]. The previous concept signifies that processes resulting in the synthesis of homogeneous glass-ceramic products, i.e. composite materials with homogeneously dispersed crystallites of similar size embedded in a residual vitreous matrix, should be enhanced. Except from the morphology, the most important physical characteristics influenced by the mechanisms of crystal phase separation are the chemical durability [4] and the mechanical properties of the final glass-ceramics [5].

Although extensive research has been devoted to some binary and ternary combinations of the above oxides, it cannot be assumed that complete knowledge has been gained. Additionally, batch compositions containing all four oxides have received scant attention so far; only postulations can be made on the ability to vitrify or on the devitrification behaviour, due to the diverse structural role of the constitutive oxides. Namely, silica (SiO_2) is a well-known vitreous network former, while sodium oxide (Na_2O) is a network modifier. Lead (PbO) and iron (Fe_2O_3) oxides are amphoteric; i.e. they can either act as network forming or network modifying oxides [6, 7]. As a result, a priori determination of the morphology of a product based on such constitutive oxides is ambiguous.

In the current work, we study the devitrification behaviour of three batch compositions of the SiO_2–Fe_2O_3–Na_2O–PbO oxides system. Initial batch compositions had equivalent SiO_2, Fe_2O_3 and PbO contents, while Na_2O was increased by small amounts. We have inspected the potential influence of small Na_2O alterations in the batch composition, due to the uncertainty in the detection of alkali ions within a vitreous matrix. This arises from the fact that alkali concentration, when detected with methods such as energy dispersive spectrometry (EDS) or microprobe analysis, exhibits higher standard deviation in relation to the elements that compose the vitreous structure or the heavier transition metal ions. This spatial inhomogeneous distribution originates from: (a) the de-alkalisation process induced from the irradiation of the electron beam [8], and (b) the inherent inhomogeneous distribution of alkali ions in a vitreous structure [9]. Therefore, modelling of a solid waste [10] can indeed elucidate crystal phase separation mechanisms that intervene to this kind of complex oxide systems.

* Presented at MEDICTA Conference 2005, Thessaloniki, peer reviewed paper.

** Author for correspondence: kehagias@auth.gr

1388–6150/$20.00

Akadémiai Kiadó, Budapest, Hungary
Springer, Dordrecht, The Netherlands

Experimental

Materials

Three batch compositions of SiO_2, Fe_2O_3, Na_2O and PbO powders were produced by mixing in such a way that the Na_2O content was gradually increased, while the quantity of the other three constituent oxides was kept constant (Table 1). The solid mixtures were placed in a Pt crucible and heated for 2 h in an electric furnace at 1400°C, at ambient atmosphere. The melt was poured on a stainless steel plate and was rapidly cooled down at room temperature. As-quenched products were pulverised and characterised by differential thermal analysis (DTA), in order to obtain the glass transition temperature (T_g) and the position of exothermic peaks that would presumably correspond to crystal phase separation [11]. DTA scans were obtained with a Setaram TG-DTA SetSys 1750°C instrument in argon atmosphere. Heating and cooling rates, for the devitrification process, were set at 10°C min^{-1} and the samples were placed in Al_2O_3 crucibles. Single-stage isothermal treatment process was applied to all as-quenched products at 700°C for 1 h.

Methods

As-quenched and annealed products were morphologically inspected by optical microscopy, using a Zeiss Axiolab-A microscope, and scanning electron microscopy (SEM) with a Jeol JSM-840A microscope, equipped with an Oxford ISIS-300 Energy Dispersive Spectrometry (EDS) analyzer. Structural characterisation was performed by X-ray diffraction (XRD) analysis with a Seifert 3003 powder diffractometer, using $CuK_{\alpha 1}$ radiation. Transmission electron microscopy (TEM) was employed for microstructural characterisation. Specimens for TEM were thinned by mechanical grinding, followed by ion-milling to reach electron transparency. TEM observations were carried out in a Jeol JEM-100CX electron microscope, operated at 100 kV.

The microhardness of as-quenched products was measured with the static indentation method with Knoop indenter geometry, using an Anton-Paar MHT-10 microhardness tester, attached on a Zeiss Axiolab-A optical microscope. The indentation parameters were set at: load=1 N, duration=10 s and loading slope=20 N s^{-1}. The loading slope was the smoothest available in order to avoid cracking during indentation. The duration of 10 s is a typical time that is long enough for the onset of plasticity. In order to resolve the indentation load that would be used for measurements, the indentation size effect (ISE) curve was obtained for all samples. The load of 1 N was found to lie in the plateau region of the ISE curve in all samples and was low enough so as to impede microcrack propagation. The microhardness values represent the mean value obtained from 12 crackless indentation prints.

Results and discussion

All batch compositions, after quenching, were transformed to non-crystalline, X-ray amorphous materials as it was verified by XRD experiments. DTA scans (Fig. 1) revealed glass transition points that are indicative of the glassy nature of the as-quenched products [12]. The glass transition points (T_g) of Synth1 and Synth2 products lie in the region of 440°C, while in the case of Synth3 product is found in the region of 420°C. TEM observations showed that the matrix of all as-quenched products lacks any detectable crystallinity down to the microscopic level. A bright

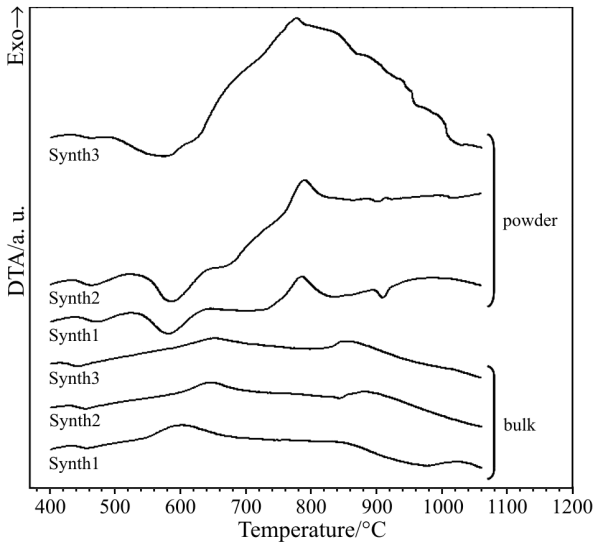

Fig. 1 DTA curves of all batch compositions in bulk and powder form

Table 1 Batch compositions (mol%), Si/O atomic ratio, microhardness (H_K) of the starting vitreous products and separated crystalline phases

Sample	SiO_2	Fe_2O_3	PbO	Na_2O	Si/O	H_K/GPa	Separated crystallites
Synth1	53.80	17.65	9.15	19.40	0.284	3.94±0.05	Fe_2O_3(H)+$FeNaSi_2O_6$
Synth2	53.15	17.45	9.00	20.40	0.283	3.85±0.06	Fe_2O_3(H)+$FeNaSi_2O_6$
Synth3	52.05	17.05	8.85	22.05	0.280	3.75±0.03	Fe_2O_3(C)

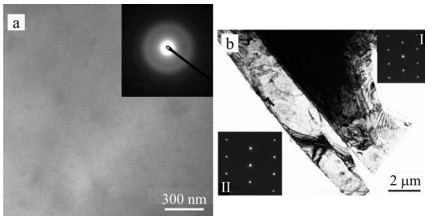

Fig. 2 a – BF TEM micrograph from as-quenched Synth1 product. The corresponding EDP is depicted in the inset; b – a hematite needle-like crystallite observed in Synth1 annealed product. The I – [1$\underline{2}$1$\underline{3}$] and II – [$\underline{2}$4$\underline{3}$4] zone axes given as insets were used to resolve the hexagonal symmetry

field (BF) TEM micrograph is shown in Fig. 2a, where a featureless matrix produces the inset electron diffraction pattern (EDP), which is characteristic of an amorphous material.

DTA scans were performed on bulk and pulverised samples in order to observe the position of exothermic peaks that possibly correspond to crystal phase separation. This is a common practice to elaborate the appropriate conditions to transform a vitreous material into a glass-ceramic and the potential influence of surface effects on the devitrification process [13]. DTA scans reveal exothermic peaks for all as-quenched pulverised samples in the region of 780°C (Fig. 1). The form of the Synth3 thermograph is different with respect to the corresponding Synth1 and Synth2 ones. However, the corresponding thermographs of bulk samples have similar profiles for all samples.

Annealing experiments were performed with identical conditions for all samples, namely at 700°C for 1 h. The morphology of annealed Synth1 and Synth2 products was similar. Needle-like crystallites were mainly dispersed in a thick surface layer (Fig. 3a), while irregularly shaped crystallites were observed only in the centre of each sample, together with crystalline needles (Fig. 3b). Annealed Synth3 morphology was different, where square shaped crystallites of similar sizes (namely of 5–10 μm) were homogeneously dispersed in the whole volume of the product (Fig. 3c). From the above, it can be deduced that the exothermic peaks above 780°C have been formed due to crystal phase separation.

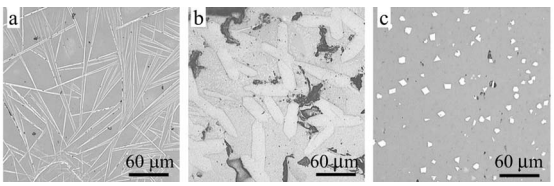

Fig. 3 Characteristic optical micrographs from Synth1 and Synth3 devitrified products: a – surface zone rich in needle-like hematite crystallites, b – acmite crystallites that have been separated in the interior of Synth1 devitrified product and c – homogeneously dispersed crystallites of maghemite in Synth3 devitrified product

The composition of the crystalline phases was found by combining EDS analyses made on numerous crystallites, XRD experiments and TEM observations. The results are listed in Table 1: Synth1 and Synth2 as-quenched products were devitrified by crystal phase separation of acmite ($NaFeSi_2O_6$) and hematite (Fe_2O_3) of hexagonal symmetry. TEM analysis revealed that hematite crystallises in the form of needle-like crystallites. Therefore, it is evident that the irregularly shaped crystallites belong to the acmite phase. Figure 2b depicts a hematite (Fe_2O_3) crystalline needle, with two EDPs that correspond to the [1$\underline{2}$1$\underline{3}$] and [$\underline{2}$4$\underline{3}$4] zone axes. Likewise, the tetragonal shaped crystallites that were observed at Synth3 devitrified product were characterised as maghemite (Fe_2O_3) of cubic symmetry.

Indentation experiments were performed to measure the microhardness values of as-quenched samples. This technique was employed to detect any potential differences between the plastic deformation mechanisms that might act in the three vitreous materials, due to the increase in Na_2O content. The results, listed in Table 1, demonstrate a tendency of the microhardness to decrease with increasing Na_2O content. Hence, both microhardness values of Synth1 and Synth2 as-quenched products are higher relative to the Synth3 one. The differences can be considered small, but still higher than the standard deviations.

A slight modification in Na_2O content produced substantial variation in the devitrification path. It was observed that DTA experiments of bulk samples, under the same conditions produced thermographs of similar profiles, while in the case of powder samples the Synth3 thermograph profile differed from the other two. As a result, it can be assumed that the difference in the crystallization sequence stems from a process that is connected to heterogeneous surface nucleation.

Needle-like hexagonal hematite (Fe_2O_3) was detected only in Synth1 and Synth2 annealed products. It has been reported that this phase originates from surface crystallisation [14] by a process that has been recognized as oxidation of Fe^{2+} to Fe^{3+}. Consequently, the difference between Synth1, Synth2 and Synth3 powder DTA profiles may be due to the lack surface nucleation of hematite in the latter, since DTA profiles are similar for all three bulk samples, where surface effects are depressed. This is also supported from the morphological observations (Fig. 3).

In the case of Synth3 product, the T_g position was found to lie 20°C below the respective T_g of Synth1 and Synth2. This emerges from the higher degree of depolymerisation of the vitreous network, induced by the increase of the Na_2O content. The fact that the microhardness value was measured to decrease with increased Na_2O shows that the vitreous

network, where plastic deformation takes place, was depolymerised to such a degree that plastic deformation mechanisms, which are based on the breakage of atomic bonds [15], were facilitated. Thus, the increase of Na_2O although limited does seem to have measurable effects on the physical properties of the as-quenched products.

Referring to the phase diagram of the SiO_2–Na_2O–Fe_2O_3 ternary system, we see that all batch compositions lie in the region, where acmite is the thermodynamically predicted crystalline phase. The separation of acmite in the inner region of Synth1 and Synth2 products is in accordance with the above observation and it seems to occur through bulk crystallisation. On the surface layer, hematite was separated through a different process, depressing the growth of acmite. This is possible since surface nucleation and growth of hematite is energetically favourable. By growing towards the interior of the sample, it consumes iron that otherwise would be used to form acmite, and finally is detained when the surface crystallisation front reaches the inner areas where acmite has already been separated.

The devitrification process of Synth3 is entirely different. The crystalline phase of maghemite has been separated in the form of homogeneously dispersed crystallites in the whole volume of the glass-ceramic. No other crystalline phase has been observed. Synth3 product is the most depolymerised one, as it is shown by the Si/O atomic ratios in Table 1. In this case, the ionic diffusion paths of the alkali ions connective tissue (Warren–Biscoe structure) possess the higher degree of interconnection. In such a structure, long-range diffusion occurs easier and bulk crystallisation is favoured over surface crystallisation [16]. Additionally, oxide systems with high concentration of iron oxide are inherently unstable, resulting to iron oxide spontaneous devitrification. It is plausible that the higher degree of interconnectivity, i.e. a change in the glass structure [17], of the alkali diffusion paths combined with the high iron oxide content triggered bulk crystallisation of maghemite.

As a more general assumption, it can be stipulated that whenever small compositional fluctuations occur, something relatively common in batch compositions containing solid wastes, they should be given special attention. Small deviations from an initial batch composition may result to products with almost indistinguishable physical properties, as in the case of Synth1 and Synth2, or to products with significantly different final microstructures after heat treatment.

Conclusions

We have studied the effect of small alkaline compositional variations to the devitrification behaviour of SiO_2–Fe_2O_3–Na_2O–PbO oxide system. It was demonstrated that small deviations in Na_2O, namely less than 2 mol%, can have measurable effects on the glass transition temperature and/or the microhardness value. Additionally, they significantly alter the devitrification mode and the composition of the separated crystalline phases. Devitrification of Synth1 and Synth2 gave rise to the growth of acmite ($NaFeSi_2O_6$) and surface crystallisation of hexagonal hematite (Fe_2O_3) phase, while separation of maghemite of cubic symmetry (Fe_2O_3) occurred in Synth3, inhibiting the growth of acmite, which is the thermodynamically predicted crystalline phase in all cases. This was attributed to the difference in surface induced effects and the influence of Na_2O content to the interconnectivity of the diffusion paths in an inherently unstable vitreous structure, rich in iron oxide.

Acknowledgements

The authors wish to acknowledge the YPEPTH and European Union for financial support through the EPEAEK II 'PYTHAGORAS II' program.

References

1 P. Kavouras, G. Kaimakamis, Th. A. Ioannidis, Th. Kehagias, Ph. Komninou, S. Kokkou, E. Pavlidou, I. Antonopoulos, M. Sofoniou, A. Zouboulis, C. P. Hadjiantoniou, G. Nouet, A. Prakouras and Th. Karakostas, Waste Manag., 23 (2003) 361.
2 P. Kavouras, Powder processing for the fabrication of advanced materials for technological applications, Ph.D. Thesis, Aristotle University of Thessaloniki, Thessaloniki 2003, p. 139.
3 Z. Strnad, Glass-Ceramic Materials, Elsevier Science Publishers, Amsterdam 1986, p. 55.
4 P. Kavouras, Ph. Komninou, K. Chrissafis, G. Kaimakamis, S. Kokkou, K. Paraskevopoulos and Th. Karakostas, J. Eur. Ceram. Soc., 23 (2003) 1305.
5 P. Kavouras, Ph. Komninou and Th. Karakostas, J. Eur. Ceram. Soc., 24 (2004) 2095.
6 J. A. Tangeman, R. Lange and L. Forman, Geochim. Cosmochim. Acta, 65 (2001) 1809.
7 C. Rüssel and A. Wiedenroth, Chem. Geol., 213 (2004) 125.
8 D. E. Clark, L. L. Hench and W. A. Acree, J. Am. Ceram. Soc., 58 (1975) 531.
9 M. D. Ingram, Glasses and amorphous materials, In Materials Science and Technology, Series, Ed. J. Zarzycki, VCH Publishers Inc., New York 1991, p. 719.
10 S. Arvelakis, F. J. Frandsen and K. Dam-Johansen, J. Therm. Anal. Cal., 72 (2003) 1005.

11 C. Tomasi, M. Scavini, A. Speghini, M. Bettinelli and M. P. Riccardi, J. Therm. Anal. Cal., 70 (2002) 151.
12 J. Zarzycki, Glasses and the vitreous state, Cambridge University Press, Cambridge 1991, p. 8.
13 C. Colella, Use of Thermal Analysis in Zeolite Research and Application. In Characterization Techniques of Glasses and Ceramics, Ed. J. Ma. Rincon and M. Romero, Springer-Verlag, 1999, p. 116.
14 A. Karamanov and M. Pelino, J. Non-Cryst. Sol., 281 (2001) 139.
15 R. H. Doremus, Glass science, John Wiley and Sons, New York 1994, p. 163.
16 P. Kavouras, Th. Kehagias, I. Tsilika, K. Chrissafis, G. Kaimakamis, D. Papadopoulos and Th. Karakostas, J. Hazard. Mater., accepted.
17 M. M. Abdel-Aziz, J. Therm. Anal. Cal., 79 (2005) 709.

Received: August 1, 2005
Accepted: October 22, 2005
OnlineFirst: June 27, 2006

DOI: 10.1007/s10973-005-7212-8